Proceedings of the Online Conference "Applications of Physics in Mechanical and Material Engineering"

Theoretical Investigation of C_3N Monolayer as Anode Material for Li/Na-Ion Batteries

G.T. Kasprzak, K.M. Gruszka and A.P. Durajski*

Institute of Physics, Częstochowa University of Technology, al. Armii Krajowej 19, 42-200 Częstochowa, Poland

Doi: 10.12693/APhysPolA.139.621 *e-mail: adurajski@wip.pcz.pl

Next-generation renewable energy technology requires electrode materials with suitable structural, electronic, and mechanical properties. Based on the *ab initio* analysis of 2D carbon and nitrogen material, we found that C_3N monolayer is one of the promising candidates for use as an anode material in Li- and Na-ion batteries. In particular, we performed first-principles calculations to investigate the geometric structure, binding energies and band structure variations of the C_3N monolayer after surface ion adsorption. We find that the Li and Na atoms prefer to stay in the hollow site among a hexagonal carbon ring and the second energetically most favorable site is the bridge site over the C–C bond. Moreover, our results demonstrate that after lithiation and sodiation, a semiconductor-to-metal transition is observed in the C_3N monolayer. The calculated theoretical capacity for Li and Na storage on the C_3N monolayer reaches 267.81 Ah/g, which indicates the potential of C_3N to be a 2D anode material for lithium- and sodium-ion batteries.

topics: C_3N, electronic properties, anode materials, DFT calculations

1. Introduction

The improvement of energy storage technologies is essential to meet the global challenge of clean and sustainable energy. To advance current rechargeable batteries further, tremendous emphasis has been put on the development of anode materials with higher capacities than the widely commercialized graphite in Li-ion batteries [1].

Two-dimensional (2D) materials are believed to be promising materials in the next-generation high-performance batteries due to their extraordinary electronic and structural properties. Very recently, attention has been turned to 2D monoatomic structures, such as graphene [2], phosphorene [3–5], borophene [6], silicene [7], stanene [8], arsenene [9], and many others. According to these studies, graphene possesses a high capacity and good cycle stability but low voltage, while phosphorene exhibits an ultrafast ion migration capability but low cycle stability and volume expansion during the charging process [10, 11]. Thus, the challenge remains to obtain a satisfactory electrode with both high capacity, superior electrical conductivity, excellent cycling stability, and good rate capability.

Recently, a 2D system consisting of carbon and nitrogen atoms (C_3N) has been successfully synthesized by Yang et al. [12]. This novel material, with a graphene-like planar structure resulting from preference to sp^2 hybridization, has aroused much interest. The material has been shown to exhibit great mechanical, thermodynamic, and electrical properties, which are beneficial for its application in various fields [13, 14]. Therefore, further examinations of its physical properties will be helpful to further exploit applications of this 2D material.

In this paper, we study the adsorption of the Li and Na ions on the surface of the C_3N monolayer through the first-principles DFT calculations. We find that the Li and Na atoms prefer to stay in the hollow site among a hexagonal carbon ring and their second most favorable site is the bridge site on the bond of C–C.

The maximum theoretical storage capacity for only partial-layer adsorption of C_3N is calculated to be 267.81 mA h/g, which is more than that of stanene, MoS_2 or NbS_2 [15]. Our computations showed that the C_3N monolayer is indeed a potential anode material for Li- and Na-ion batteries.

2. Computational methods

To study the electronic properties of the investigated material, first-principles calculations are performed within the framework of the density-functional theory (DFT) [16] as implemented in the Quantum Espresso package [17]. The generalized gradient approximation of Perdew–Burke–Ernzerhof (GGA-PBE) is used for the exchange-correlation functional together with the projector-augmented wave (PAW) method. A plane-wave basis set with kinetic energy cutoff is set as 90 Ry

to ensure the accuracy of simulation results. A vacuum of 20 Å along the z axis was applied to prevent interlayer interactions from periodic images.

The optimized atomic structures were obtained by fully relaxing both atomic positions as well as cell parameters by using the Broyden–Fretcher–Goldfarb–Shanno (BFGS) quasi-Newton algorithm until all forces are smaller than 0.01 eV/Å. The Brillouin zone is sampled utilizing a $20\times20\times1$ k-mesh in the Monkhorst–Pack scheme. After structural optimization, the density of states (DOS) and electronic properties are calculated using the denser $60\times60\times1$ Monkhorst–Pack grid.

3. Results and discussion

The crystal structure of the C_3N monolayer has a $P6/mmm$ symmetry with a hexagonal lattice. The optimized lattice constants are $a = b = 4.8627$ Å. As in the case of graphene, C_3N has a flat structure due to the fact that all C and N atoms are sp^2 hybridized. In our calculations, as shown in Fig. 1a, six highly symmetric adsorption sites on the C_3N surface are modeled: a hollow site among six carbon atoms (H^C), a hollow site among four carbons and two nitrogen atoms (H^{CN}), a top site of the carbon atoms (T^C), a top site of the nitrogen atoms (T^N), a bridge site of the carbon-carbon atoms (B^C), and finally a bridge site of the carbon-nitrogen atoms (B^{CN}).

During the relaxation, we restricted both the Li and Na atoms movement, allowing only a perpendicular motion to the surface in order to keep them above these initial positions. It is shown that the structure with both the Li and Na atoms at the H^C site is the most stable because it has the lowest

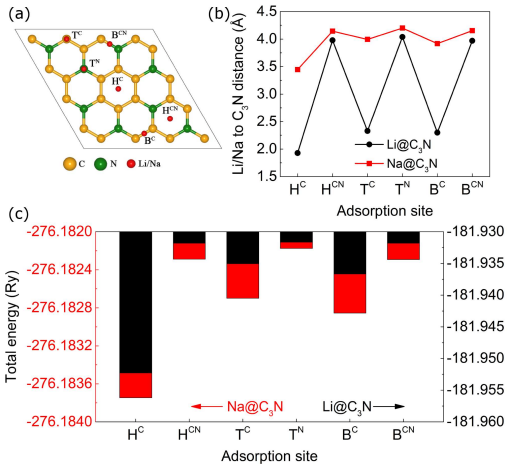

Fig. 1. (a) Six different adsorption sites on the C_3N surface. The orange, green and red spheres represent carbon, nitrogen and lithium or sodium atoms, respectively. (b) Vertical distances between the adatom and the surface of C_3N at different sites. (c) Total energy of C_3N with the Li/Na adatom at different sites.

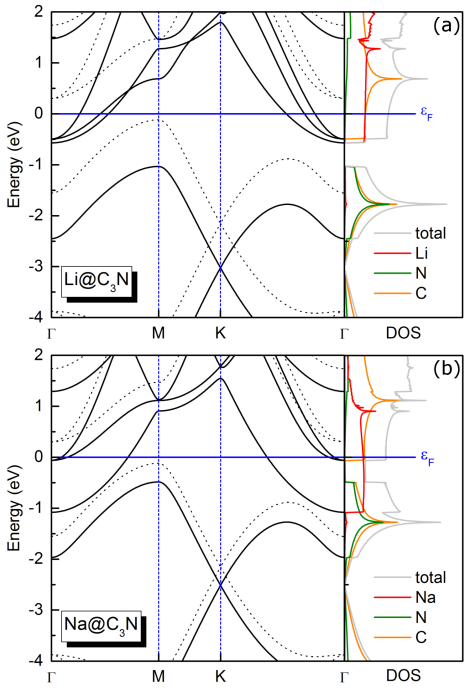

Fig. 2. Electronic band structure and DOS of C_3N with Na (a) and Li (b) atom adsorbed at the hollow site among a hexagonal carbon ring. The Fermi level is marked by the horizontal blue line. The dotted bands are for the pristine C_3N monolayer.

total energy among all other studied sites and the shortest adatom–surface distance (see Fig. 1b and c) which typically means stronger bonding. The second most favorable site is the bridge site on the top of a C–C bond. It is also worth noting that the bonding character in both ion cases for H, T and B sites is similar, showing the same energetic tendency.

For energetically most stable case, the band structure and density of states (DOS) have been calculated to investigate the electronic properties of C_3N after lithiation and sodiation. The pristine C_3N exhibits a semiconducting behavior with the indirect band gap of 0.42 eV between M and Γ points in the Brillouin zone which limits its electrochemical performance.

As presented in Fig. 2, the change of the electronic band structure of C_3N upon the Li or Na ions adsorption, implies a semiconducting-to-metallic transition due to the presence of bands crossing the Fermi level. This provides considerable electronic conductivity required for electrode materials. However, the transition mechanism in both cases is different what can be seen by looking at DOS plots, where Na, in contrast to Li, is responsible for providing more additional states below the Fermi level. This is also manifested by a visible band starting around -1 eV at Γ point. Despite this, the DOS character in both cases is similar; below ε_F DOS consists mainly of N and C states while near and above ε_F visible is the mixing of Li/Na and C states.

TABLE I

The calculated total energies (E) and binding energies (E_b) for C_3N with Na or Li adsorbed atom.

Site	E_{C_3N+Na} [Ry]	E_{C_3N+Li} [Ry]	E_b^{Na} [eV]	E_b^{Li} [eV]
H^C	−276.1837	−181.9523	0.0479	0.3090
H^{CN}	−276.1823	−181.9318	0.0281	0.0303
T^C	−276.1827	−181.9350	0.0337	0.0744
T^N	−276.1822	−181.9316	0.0265	0.0281
B^C	−276.1828	−181.9367	0.0358	0.0964
B^{CN}	−276.1823	−181.9318	0.0281	0.0304

The binding energy (E_{rmb}) of the adsorbed Li and Na atoms on the C_3N monolayer is defined as [18]:

$$E_b = \frac{E_{C_3N} + nE_M - E_{C_3N+M}}{n}, \quad (1)$$

where E_{C_3N+M} and E_{C_3N} are the total energies of C_3N with and without the adsorbed atom (M = Li or Na), respectively, E_M — the energy of the isolated Li or Na atom and n — the number of absorbed Li/Na atoms. According to this definition, a larger value of E_b indicates a stronger interaction between Li/Na and the C_3N monolayer.

As we can see in Table I, in all cases the binding energy is positive, which means that the Li and Na ions can be absorbed on the C_3N surface, and, moreover, the largest values obtained at the hollow site among the hexagonal carbon ring indicate the strongest interaction at this position.

The open circuit voltage (OCV) is an important indicator of the performance of the anode material. Note that the binding energy defined here can also be interpreted as the OCV if the entropy effects are neglected [19]. The OCV of a commercial anode should be lower than 0.8 V to have enough high cell voltage, but not too close to zero to avoid dendrite formation on the anode surface. Here, the voltage of 0.31 V for Li at the H^C site is thus quite suitable.

In order to compare the tested material with other anode materials, the storage capacities ware calculated by using [20]

$$C = \frac{exN_A}{\varepsilon M_{C_3N}}, \quad (2)$$

where N_A is the Avogadro constant, x is the concentration of ions, e is the elementary charge, ε is the conversion ratio ($\varepsilon = 3.6$ C/(mA h)), and M_{C_3N} is the molar mass of the substrate (50.04 g/mol).

In this paper, only partial-layer adsorption (the concentration of $M_{0.5}C_3N$) was assumed for Li and Na atoms, resulting in a relatively small capacity of 267.82 mA h/g, which is lower than that of the commercially used graphite-based batteries (372 mA h/g) but higher than, e.g., for stanene (226 mA h/g), NbS_2 (265 mA h/g) or MoS_2 (146 mA h/g) [15]. Further researches focusing on the increase of Li/Na ion concentration are needed for a more detailed examination of the potential application of C_3N as an anode material.

4. Conclusions

First-principles calculations based on the density functional theory have been carried out to investigate the adsorption of Li and Na atoms on C_3N monolayer to explore its potential applications as anode material in Li- and Na-ion rechargeable batteries.

Our calculations showed that the optimal adsorption site of the Li/Na ions on C_3N is the hollow site above the center of the carbon hexagon. A transition from semiconducting to metallic state upon lithiation/sodiation and theoretical capacity of 267.82 mA h/g reveal the potential of the C_3N monolayer to be appropriate for use as the anode material.

Acknowledgments

This research was partly supported by PL-Grid Infrastructure.

References

[1] K. Sato, M. Noguchi, A. Demachi, N. Oki, M. Endo, *Science* **264**, 556 (1994).

[2] K.S. Novoselov, A.K. Geim, S.V. Morozov, D. Jiang, Y. Zhang, S.V. Dubonos, I.V. Grigorieva, A.A. Firsov, *Science* **306**, 666 (2004).

[3] A. P. Durajski, K.M. Gruszka, P. Niegodajew, *Appl. Surf. Sci.* **532**, 147377 (2020).

[4] A. Khandelwal, K. Mani, M.H. Karigerasi, I. Lahiri, *Mat. Sci. Eng.: B* **221**, 17 (2017).

[5] M. Alidoust, M. Willatzen, A.-P. Jauho, *Phys. Rev. B* **99**, 125417 (2019).

[6] A.J. Mannix, X.-F. Zhou, B. Kiraly et al., *Science* **350**, 1513 (2015).

[7] H. Oughaddou, H. Enriquez, M.R. Tchalala, H. Yildirim, A.J. Mayne, A. Bendounan, G. Dujardin, M. Ait Ali, A. Kara, *Prog. Surf. Sci.* **90**, 46 (2015).

[8] J.-K. Lyu, S.-F. Zhang, C.-W. Zhang, P.-J. Wang, *Ann. Phys.* (Berlin) **531**, 1900017 (2019).

[9] J. Shah, W. Wang, H. M. Sohail, R.I.G. Uhrberg, *2D Materials* **7**, 025013 (2020).

[10] J. Zhu, G. Xiao, X. Zuo, *Nano-Micro Lett.* **12**, 120 (2020).

[11] H.F. Xiang, Z.D. Li, K. Xie, J.Z. Jiang, J.J. Chen, P.C. Lian, J.S. Wu, Y. Yu, H.H. Wang, *RSC Adv.* **2**, 6792 (2012).

[12] S. Yang, W. Li, C. Ye et al., *Adv. Mat.* **29**, 1605625 (2017).

[13] X. Zhou, W. Feng, S. Guan, B. Fu, W. Su, Y. Yao, *J. Mater. Res.* **32**, 2993 (2017).

[14] G.-C. Guo, R.-Z. Wang, B.-M. Ming, C. Wang, S.-W. Luo, M. Zhang, H. Yan, *J. Mater. Chem. A* **7**, 2106 (2019).

[15] J. Li, G. Tritsaris, X. Zhang et al., *J. Electrochem. Soc.* **167**, 090527 (2020).

[16] R. Parr, W. Yang, *Density-functional theory of atoms and molecules*, Oxford University Press, New York 1989.

[17] P. Giannozzi, O. Andreussi, T. Brumme et al., *J. Phys. Condens. Matter.* **29**, 465901 (2017).

[18] X. Fan, W. Zheng, J.-L. Kuo, *ACS Appl. Mater. Interfaces* **4**, 2432 (2012).

[19] S. Zhao, W. Kang, J. Xue, *J. Mater. Chem. A* **2**, 19046 (2014).

[20] H. Liu, H. Dong, Y. Ji, L. Wang, T. Hou, Y. Li, *Appl. Surf. Sci.* **466**, 737 (2019).